Available online at www.sciencedirect.com
ScienceDirect
Precambrian Research 157 (2007) 106–126
Precambrian Research
www.elsevier.com/locate/precamres

Proterozoic metamorphism and cooling in the southern Lake Superior region, North America and its bearing on crustal evolution

D.K. Holm [a,*], D.A. Schneider [b], S. Rose [b], C. Mancuso [a], M. McKenzie [a], K.A. Foland [c], K.V. Hodges [d,1]

[a] *Department of Geology, Kent State University, Kent, OH 44242, USA*
[b] *Department of Geological Sciences, Ohio University, Athens, OH 45701, USA*
[c] *Department of Geological Sciences, Ohio State University, Columbus, OH 43210, USA*
[d] *Department of Earth, Atmospheric & Planetary Sciences, Massachusetts Institute of Technology, Cambridge, MA 02139, USA*

Received 14 April 2006; received in revised form 5 November 2006; accepted 5 February 2007

Abstract

Metamorphism along the southern margin of the Archean Superior Province has been historically attributed to the Penokean orogeny. A narrow corridor of amphibolite facies rocks north of the main suture does record 1.83–1.80 Ga metamorphic monazite U–Th–Pb ages that mark the culmination of arc accretion. However, subsequent widespread amphibolite facies metamorphism and associated magmatism is recorded along the regions of greatest Penokean crustal thickening: the tectonically buried Archean–Proterozoic continental margin. In Minnesota, new monazite geochronology reveals a profound midcrustal metamorphic imprint caused by emplacement of the ~1.775 Ga East-central Minnesota batholith at moderate depths. In northern Wisconsin and upper peninsula Michigan metamorphic monazite growth at 1.78–1.745 Ga (and far from geon 17 intrusions) reflect a previously little recognized regional amphibolite facies metamorphic event associated with ca. 1.76 Ga Yavapai-interval accretion, not solely Penokean induced crustal collapse.

South of the Penokean suture, Penokean terrane rocks were twice metamorphosed to upper greenschist facies; first during Yavapai accretion and again during geon 16 Mazatzal accretion. Geon 16 overprinting also affected a small part of the continental margin in the northeast orogen, the Peavy metamorphic node. South-directed basement thrusts there likely accommodated substantial Mazatzal foreland shortening, suggesting thick-skinned deformation. Mazatzal amphibolite facies metamorphism occurred throughout Iowa and southernmost Wisconsin (south of the Baraboo quartzite).

$^{40}Ar/^{39}Ar$ mineral cooling ages from eastern Wisconsin reveal a limited metamorphic aureole associated with the intrusion of the 1.47 Ga Wolf River batholith, in part reflecting its rapid emplacement at shallow crustal levels. A local area of anomalously young <1.20 Ga $^{40}Ar/^{39}Ar$ mica ages away from known Midcontinent Rift exposures probably reflect shallow crustal level reheating during rifting, not exhumation.

The pattern and degree of Proterozoic metamorphism preserved across the northern interior of the North American midcontinent is highly variable and is a reflection of multiple accretionary and intrusive events between 1.87 and 1.47 Ga. Collectively, the geo- and thermochronologic data reveal a progressive tectonic younging toward the south and overall waning of Proterozoic metamorphism

* Corresponding author. Tel.: +1 330 672 4094.
E-mail address: dholm@kent.edu (D.K. Holm).
[1] Current address: School of Earth and Space Exploration, Box 871404, Arizona State University, Tempe, AZ 85287-1404, USA.

0301-9268/$ – see front matter
doi:10.1016/j.precamres.2007.02.012

in this region. These results demonstrate a changing tectonic environment from active margin to continental interior as Laurentia grew southward and stabilized over a few hundred million years.

Keywords: Proterozoic; Geochronology; Thermochronology; Metamorphism

1. Introduction

The exposed bedrock of the north-central United States presents a unique perspective into the Precambrian evolution of the North American lithosphere. Now known to comprise a mosaic of southward younging Paleoproterozoic juvenile arcs similar to that of the southwest U.S. (Fig. 1; NICE working group, 2007), the Upper Great Lakes region has remained tectonically undisturbed for the last one billion years. This area thus presents a rare opportunity to examine the thermal evolution of cratonic crust from its inception as an active arc system through its maturation into stable continental interior.

New geochronologic data support the interpretation that late Paleoproterozoic crust in the northern midcontinent represents eastward continuation of the geon 17 and 16 Transcontinental Proterozoic Provinces in the southwest U.S. (Van Schmus et al., 2007). Multiple Proterozoic orogenic and magmatic events were responsible for forming and shaping the present crustal and lithospheric structure of the region. Determining the timing and extent of associated metamorphism has been essential for unraveling its complex geologic history. In this paper we present new U–Th–Pb metamorphic geochronometric and $^{40}Ar/^{39}Ar$ thermochronometric data which place temporal constraints on the protracted tectonothermal evolution of the ancient margin and document the differing thermal influences of two notable Proterozoic batholiths. Collectively, our new data reflect a changing tectonic environment from hot orogenic margin to cold continental interior—a change that is reflected by an overall waning of Proterozoic metamorphism in this region.

2. Geologic setting

The bulk of Laurentia (northern United States and Canada) formed by aggregation of Archean continents and juvenile arcs at ca. 1900–1800 Ma during the Trans-Hudson and Penokean orogenies (Hoffman, 1989). Subsequent accretion of arc terranes along the southern margin of Laurentia formed the Transcontinental Proterozoic Provinces (Van Schmus et al., 1993),

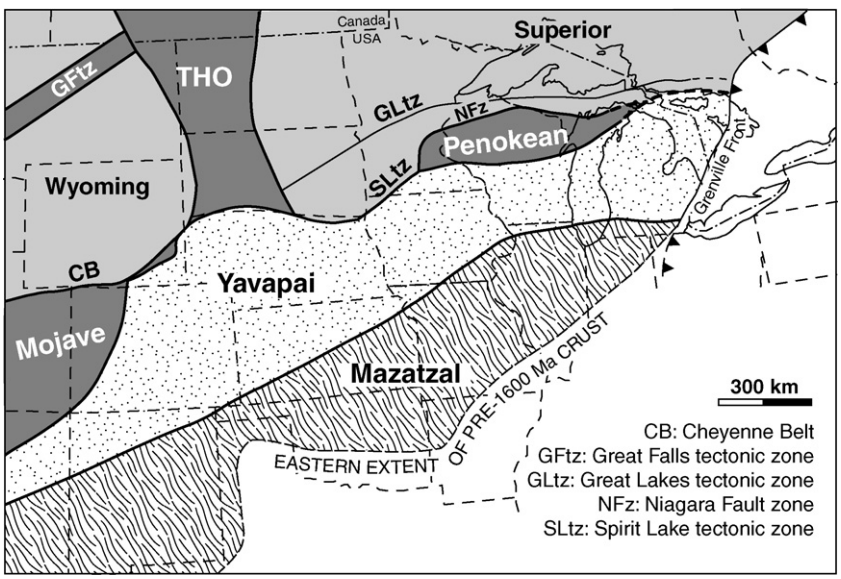

Fig. 1. Tectonic province map of the North American midcontinent, which represents Laurentia at ca. 1600 Ma and shows major Archean (Wyoming and Superior) and Paleoproterozoic provinces (after Van Schmus et al., 1993; NICE working group, 2007). Grenville Front shown to illustrate the truncation of the provinces to the northeast. THO: Trans-Hudson orogen.

which broadly consist of a northern 1800–1700 Ma inner accretionary belt (i.e., Yavapai orogen) and a southern 1700–1600 Ma outer accretionary belt (i.e., Mazatzal orogen; Karlstrom et al., 2001).

In the southern Lake Superior region, the Paleoproterozoic Penokean orogeny (1875–1835 Ma; Van Schmus, 1976, 1980) represents an island/back-arc and micro-continent/continent collision that deformed and metamorphosed Archean basement and Paleoproterozoic continental margin rocks. The steep, south-dipping Niagara fault zone is an 1860 Ma suture that separates the northern deformed continental margin rocks from the juvenile Wisconsin magmatic terrane (Fig. 2; Larue, 1983). In central Wisconsin, the steep, south-dipping Eau Pleine shear zone separates these same magmatic arc rocks from the Archean Marshfield terrane to the south. The Penokean orogeny culminated around 1835 Ma, as demonstrated by several undeformed granites of that age which pierce these main sutures and adjacent thrust sheets (Sims et al., 1989; Schneider et al., 2002).

The deepest exposed Paleoproterozoic metamorphic rocks occur within a belt of gneiss domes that lies immediately north of the Niagara fault zone. In east-central Minnesota (Fig. 2), metamorphic grade increases evenly toward the south from essentially nonmetamorphosed Paleoproterozoic sedimentary rocks (Animikie basin) through higher temperature isograds of the medial zone (up to staurolite zone at 6–7 kb) to where upper amphibolite facies metamorphism is reached in the plutonic-internal zone south of the Malmo structural discontinuity and the McGrath gneiss dome (Fig. 2; Holm and Selverstone, 1990). The southward increase in metamorphic conditions and change in deformational style (Holst, 1984; Southwick et al., 1988) is considered to reflect an increase in depth of exposure from foreland to internides of the deeply eroded ancient Penokean orogenic architecture. The relation between gneiss dome formation and metamorphism in northern Michigan has long captured the interest of geologists since subcircular metamorphic isograds where first described there by James (1955). Imparted on this area are a southerly elliptical series of isograds known as the Peavy metamorphic node, culminating in the sillimanite zone at 4 kb, and a larger northerly, more concentric series of 'bullseye' isograds called the Republic metamorphic node, peaking in the andalusite zone at 2–3 kb (Attoh and Klasner, 1989). Both nodes are distinctly associated with exhumed domes of Archean basement (Marshak et al., 1997; Schneider et al., 2004). In northern Wisconsin, structural panels of strongly deformed and metamorphosed Paleoproterozoic metasedimentary rocks occur subparallel to the Niagara fault zone, containing greenschist facies to kyanite/sillimanite zone assemblages (Cannon and Ottke, 2000; Schneider et al., 2004). The accreted Wisconsin magmatic terrane preserves dominantly upper greenschist facies metamorphism, except locally where intruded by younger plutons.

Following geon 18 accretion, the internides of the Penokean orogen again became the locus of arc magmatism triggered by renewed subduction, recorded as pulses of plutonism at ca. 1800, 1775, and 1750 Ma likely due to Yavapai-interval convergence (Holm et al., 2005). Geon 17 magmatism was concurrent with gneiss dome formation and significant crustal exhumation in the aforementioned corridor of deformed rocks north and west of the Niagara fault zone, and immediately preceded a ca. 100 million years period of tectonic quiescence across the region (Schneider et al., 2004; Holm et al., 2005). The newly identified Spirit Lake tectonic zone represents an accretionary boundary separating Penokean terrane rocks (north) from dominantly juvenile Yavapai arc rocks to the south (NICE working group, 2007; Van Schmus et al., 2007)

The ca. 1700 Ma Baraboo Interval quartzite blanketed the orogenic belt succeeding geon 17 magmatism (Dott, 1983; Holm et al., 1998b; Medaris et al., 2003). Shortly after deposition of the Baraboo-interval quartzite, most of the rocks of the Wisconsin magmatic terrane were deformed and thermally reheated during Mazatzal-interval arc accretion at ca. 1650–1630 Ma (Holm et al., 1998b). The northern extent of Mazatzal overprinting in northern Wisconsin (Fig. 2) is subparallel to the Niagara fault zone and is delineated by both a deformational front in the Baraboo-interval quartzite and a thermal (isotopic resetting) front in the underlying basement rocks (Holm et al., 1998b).

Southward Paleoproterozoic growth of Laurentia was followed by a prolonged period of Mesoproterozoic (geons 13 and 14) post-aggregation magmatism, with large volumes of dominantly granitoid intrusions emplaced along a belt extending from California to Scandinavia (Anderson, 1983). The 1470 Ma Wolf River batholith of central Wisconsin (Fig. 2) is one of the older intrusions of this transcontinental igneous province. Emplacement of the batholith was apparently the final step in the cratonization of this portion of Laurentia (Rogers et al., 1984; Allen and Hinze, 1992; Holm and Lux, 1998; Romano et al., 2000). A subsequent attempt to rift Laurentia at 1100 Ma failed, imparting relatively little effect on the crust away from the midcontinent rift axis (NICE working group, 2007).

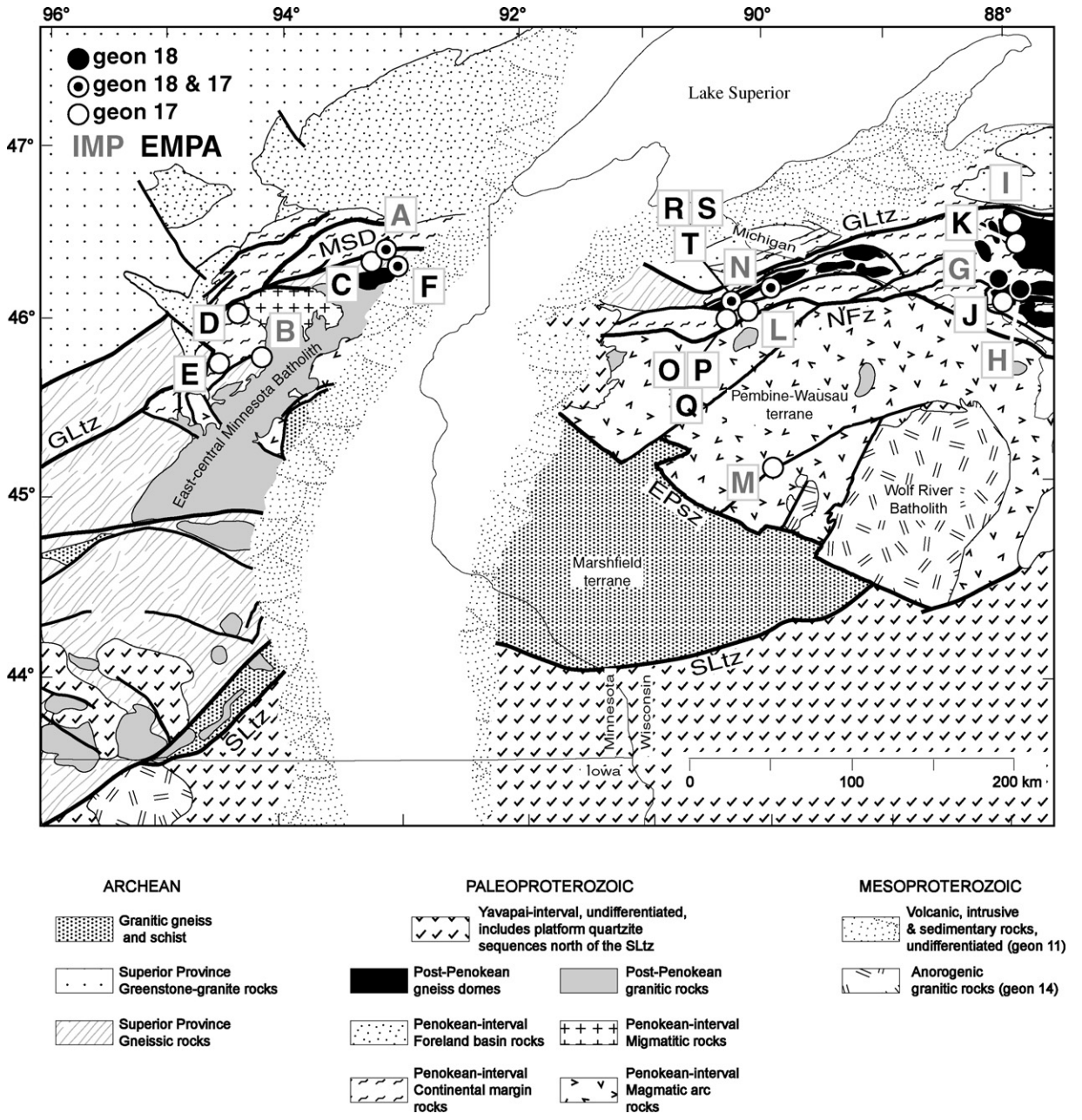

Fig. 2. Precambrian geology map of the western Lake Superior region, with locations of samples for monazite geochronology (letters correspond to Table 1). Location labels and color are categorized by age and technique. Farthest west gneiss dome in MN (solid black) is the McGrath gneiss dome; farthest gneiss dome to the northeast MI is the Republic gneiss dome, and to the south of Republic are domes associated with the Peavy region. GLtz: Great Lakes tectonic zone; EPsz: Eau Pleine shear zone; SLtz: Spirit Lake tectonic zone. MSD: Malmo structural discontinuity; NFZ: Niagara fault zone.

3. Previous geochronology

Early midcontinent geochronologic studies by Goldich et al. (1961, 1970), Aldrich et al. (1965), and Peterman (1966) were pioneering applications of radiometric dating which provided a broad-brush means of correlation and contributed to the initial formation of a world-wide time scale for the Precambrian (Goldich, 1968). Biotite Rb/Sr ages compiled for Wisconsin and northern Michigan range from ca. 1750 to 1100 Ma

(Peterman and Sims, 1988). A locus of anomalously young Rb/Sr dates (1100–1200 Ma) in northeast Wisconsin was interpreted as recording flexural uplift associated with lithospheric loading by midcontinent rift volcanic rocks to the north. The remaining biotite Rb/Sr ages increase erratically away from the young locus in all directions.

Over the past decade, a growing dataset of modern $^{40}Ar/^{39}Ar$ thermochronometric ages from the southern Lake Superior region has revealed important information on the timing and degree of metamorphism and postmetamorphic cooling across the orogenic belt (recently reviewed in Schneider et al., 2004). The number of geon 18 Penokean-interval cooling ages is few (Schneider et al., 1996; Holm et al., 2005); the majority of mineral $^{40}Ar/^{39}Ar$ dates from both geon 17 plutons and deformed country rock being 1760 and 1700 Ma (Holm and Lux, 1996; Holm et al., 1998b), a reflection of widespread cooling from Yavapai-interval plutonism and amphibolite-facies metamorphism. With the exception of Romano et al. (2000), most published thermochronometric results are from the region of highest Paleoproterozoic metamorphic grade north (northern Michigan and Wisconsin) and west (east-central Minnesota) of the Niagara fault zone. Holm et al. (1998a) and Romano et al. (2000) illustrated that lower grade regions south of the Niagara fault zone and east of the midcontinent rift were deformed and variably metamorphosed during ca. 1650 Ma Mazatzal-interval accretion, but little affected after that. In contrast, Medaris et al. (2003) have proposed that the Wolf River batholith imposed a geographically widespread, but stratigraphically localized, hydrothermal imprint along the sub-Baraboo Interval quartzite nonconformity.

Few studies have attempted to directly constrain the timing of peak Proterozoic metamorphism is the Lake Superior region, with much of the metamorphism historically attributed to the Penokean orogeny (Goldich et al., 1961; Geiger and Guidotti, 1989). However, recent application of modern radiometric techniques, particularly of U–Th–Pb monazite dating using both ion and electron microprobe techniques, allow recognition of distinct metamorphic pulses at 1835 Ma, 1800 Ma, and ca. 1770 Ma—metamorphic ages which are directly tied to known magmatic events (Schneider et al., 2004; Holm et al., 2005). This paper presents results that expand our previous metamorphic monazite geochronology, and reports new $^{40}Ar/^{39}Ar$ incremental mineral cooling ages from the eastern orogen, complemented by Ar laser microprobe ages on selected muscovite grains across the region.

4. Analytical methods

4.1. U–Th–Pb monazite geochronometry

In order to constrain the timing of moderate to high temperature metamorphism of the southern Lake Superior region, primarily *in situ* ion microprobe $^{232}Th/^{208}Pb$ and $^{207}Pb/^{206}Pb$ geochronometry and complimentary *in situ* electron microprobe total-Pb monazite geochronometry were applied to metamorphic units from Minnesota, Wisconsin, and Michigan. Monazite was principally chosen for analysis because the mineral contains large amounts of Th and U, has minor ^{204}Pb, and exhibits little elemental diffusion under high-temperatures (Catlos et al., 2002). Furthermore, monazite is ideal for studying polyphased tectonometamorphic histories because of its high closure temperature (>850 °C; Cherniak et al., 2004) and ability to preserve multiple thermal events in elemental zoning patterns within the crystal (Townsend et al., 2000). Upper greenschist to amphibolite facies Archean basement and Proterozoic supracrustal units were sampled to determine geographic and structural variability of metamorphism across the orogen. Schneider et al. (2004) presented metamorphic age results obtained through similar methodologies, and this contribution augments and fully develops those existing data. Collectively, the sample locations selected provide a thorough coverage of the major metamorphic features found across the western Lake Superior region (Fig. 2).

Monazite multiple-spot, single-grain $^{232}Th/^{208}Pb$ and $^{207}Pb/^{206}Pb$ ages were measured using the Cameca ims1270 ion microprobe facility at the University of California, Los Angeles following the protocol described by Catlos et al. (2002). Prior to analysis, monazite grains were located in thin sections, imaged with BSE/SEM techniques, drilled out, and mounted with an age-standard in an epoxy probe mount. For isotopic analyses, the primary ion beam is O^- and was focused to a 13 μm × 18 μm spot. The standard operating conditions were a primary intensity of 3–4 nA, mass resolving power of ~4500 and a 50 eV energy window. The Th–Pb monazite ages were determined relative to the monazite standard 554 (45 ± 1 Ma; Harrison et al., 1999). The precision of the method is not limited by counting statistics but by the reproducibility of the standard calibration curve which is typically ±1–2% (Harrison et al., 1995). Thorium concentrations were estimated semiquantitatively by comparing peak heights in the unknowns to that in the standard 554, with a mean concentration of ~40,000 ppm. Due to the heterogeneity of U in standard 554, only Th can be utilized for the calculations.

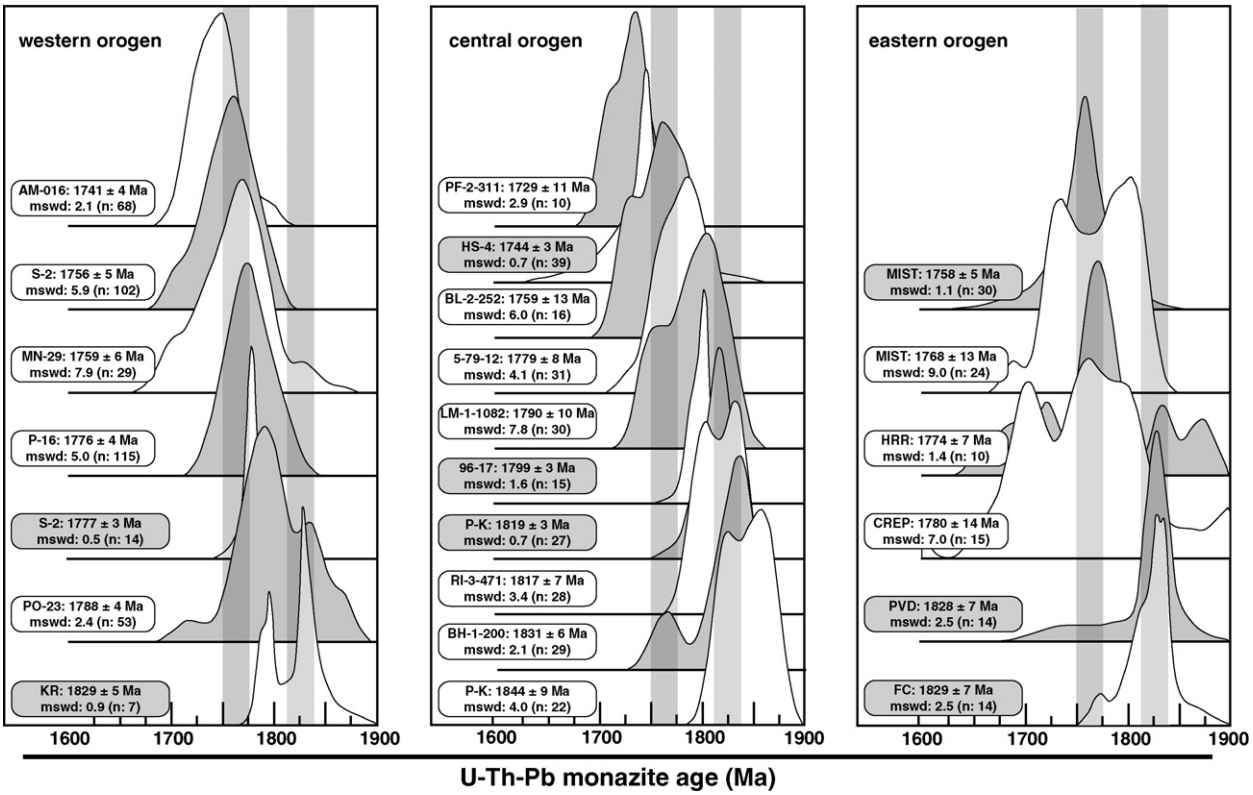

Fig. 3. Monazite U–Th–Pb relative probability curves based on single-spot electron microprobe total-Pb analysis (white data boxes) and single-spot ion microprobe $^{207}Pb/^{206}Pb$ analysis (shaded data boxes). Vertical gray bars illustrate timing of ca. 1830 Ma Penokean-interval metamorphism and 1775–1750 Ma Yavapai-interval metamorphism. Ages are from this study and U–Pb ages from Schneider et al. (2004), and are summarized in Table 1. See text for treatment of data; peak heights are not normalized.

In situ ion microprobe geochronology was performed on six metapelitic and gneissic rocks, averaging two spots per monazite, although this was limited by the size and irregular shape of many crystals. Accessory mineral isotopic ages and errors ($\pm 1\sigma$) were reduced and calculated based on the methods of Harrison et al. (1995) and Catlos et al. (2002); Table A1 includes detailed isotopic analyses available as electronic supporting material. Unfortunately, the Th–Pb analyses yielded unreliable dates, often with large errors, even though the monazite contained significant radiogenic ^{208}Pb; thus, our results focus on the more reliable $^{207}Pb/^{206}Pb$ ages. Single-spot $^{207}Pb/^{206}Pb$ dates were then plotted on relative probability diagrams through Isoplot to assess the major populations of mineral-age domains for a given sample, shown as 'peaks' in Fig. 3. Once populations were identified, $^{207}Pb/^{206}Pb$ dates were plotted on weighted average diagrams in order to calculate domain age and error, applying the well-established convention of maintaining a mean square weighted deviation (MSWD) below 2.5 for a given population (Table 1).

The *in situ* chemical U–Th–total Pb dating technique was also employed on monazite from eight samples across the orogen using the electron microprobe analyzer (EMPA; Suzuki and Adachi, 1991; Montel et al., 1996; Cocherie et al., 1998; Williams et al., 1999). Three of these samples were also dated via the ion microprobe method, in part to assess the reliability of the EMPA dates, but also to take advantage of the electron microprobe's 5 μm beam diameter (versus that of the ion microprobe at >15 μm) for higher-spatial intracrystalline analyses. This EMPA portion of the investigation involved two techniques: high-resolution compositional mapping to aid in the identification of intracrystalline age domains, and quantitative chemical analyses of Y, Th, U, and Pb. Analyses were carried out on a Cameca SX-50 electron microprobe at the University of Massachusetts-Amherst. Monazite grains were identified through manual scanning of rock thin sections noting high Ce-peaks, in addition to using energy dispersion spectra (EDS). Images were collected using high sample current (>200 nA) and small step sizes (~0.5 μm), while rastering the electron beam with the stage fixed (50 ms

Table 1
Summary of U–Th–Pb metamorphic monazite ages, western Lake Superior

Sample	Map reference	UTM	Lithology	Pb/Pb age[a] (Ma)	± (Ma)	MSWD	n[b]	Total Pb age[a] (Ma)	± (Ma)	MSWD	n[b]
Western orogen (Minnesota)											
KR[c]	A	15 508969E 5137425N	gt + st schist	1829	5	0.9	7				
				1793	4	1.0	4				
S-2	B	15 406541E 5053782N	bio gneiss	1777	3	0.5	14	1756	5	5.9	102
AM-016	C	15 468009E 513211 1N	st schist					1741	4	2.1	68
MN-29	D	15 394502E 5079299N	st schist					1759	6	7.9	29
P-16	E	15 392490E 5077998N	gt + st schist					1776	4	5.0	115
PO-23	F	15 511658E 5147828N	gt + st schist					1844	7	2.5	28
								1788	4	2.4	53
Eastern orogen (Michigan)											
PVD	G	16 406511E 5093247N	mica schist	1828	7	2.5	14				
FC[c]	H	16 443853E 5090257N	Archean schist	1829	5	2.1	17				
MIST	I	16 412714E 5151335N	st schist	1758	5	1.1	30	1768	13	9.0	24
HRR	J	16 402029E 5093598N	Archean gneiss					1774	7	1.4	10
CREP	K	16 423710E 5136192N	Archean gneiss	2576	18	16.0		2577	19	12.0	15
								1780	14	7.0	15
Central orogen (Wisconsin)											
96-17	L	15 568556E 5181479N	mica schist	1799	3	1.6	15				
HS-4	M	16 266771E 4994533N	gt schist	1744	3	0.7	39				
P-K[c]	N	15 731671E 5107288N	ky schist	1819	3	0.7	27	1844	9	4.0	22
				1791	6	1.2	8				
PF-2-311[c]	O	15 696244E 5089876N	gt + sil schist					1729	11	2.9	10
BL-2-252[c]	P	15 686125E 5088839N	gt + sil schist					1759	13	6.0	16
5-79-12[c]	Q	15 691586E 5079075N	gt schist					1779	8	4.1	31
RI-3-472[c]	R	15 702097 E5093513N	ky + st schist					1817	7	3.4	28
LM-1-1082[c]	S	15 730347E 5119394N	ky + st schist					1790	10	7.8	30
BH-1-200[c]	T	15 706892E 5092162N	gt schist					1831	6	2.1	29
								1764	8	0.9	7

[a] Pb/Pb age determined from ion microprobe analyses, total Pb age determined from EMPA analyses.
[b] Number of analytical spots.
[c] Re-calculated data presented in Schneider et al. (2004).

per pixel resolution of 512 × 512 pixels). Elemental maps were analyzed for distinct chemical domains to determine optimal transect placement for age determinations; analytical protocol was carried out following Williams and Jercinovic (2002) and Schneider et al. (2004), and detailed in Rose (2004). Matrix corrections were done using the PAP method of Pouchou and Pichoir (1984, 1985). Quantitative trace-element analysis was done using a beam current of 150–200 nA at 15 kV accelerating voltage with a counting time of 700–900 s. Once concentrations of U, Th, and Pb were obtained, the age equation of Montel et al. (1996) was solved by iteration based on calculated Pb (Table A2 includes detailed elemental analyses available as electronic supporting material).

After single-spot total-Pb ages were calculated as described above, age populations were assessed with Isoplot similar to the method outlined for the ion microprobe data. Up to 84 spots on each sample were collected, specifically targeting Th-rich rims and lower-Th cores. Total-Pb ages and errors presented may only reflect analytical precision (analyses are grouped by identified domains) and were calculated using the equation for standard error of the mean based on the number of analyses for each domain. Weighted-mean ages were calculated using the standard error from individual analyses of similar age domains and reported at the 2σ level (Fig. 3 and Table 1). For consistency with respect to discussing our new age data in the context of previously reported total-Pb monazite ages from the orogen, we also re-reduced the total-Pb dates presented in Schneider et al. (2004) in a similar manner (Fig. 3 and Table 1).

4.2. $^{40}Ar/^{39}Ar$ thermochronometry

Archean basement and Proterozoic supracrustal and intrusive units were collected from outcrops and roadcuts in eastern Wisconsin and the western part of Michi-

gan's Upper Peninsula. Thin sections were examined to evaluate their suitability for dating; samples containing the desired minerals and exhibiting little or no alteration were then crushed, sieved, and ultrasonically cleaned, rinsed, and dried. Mica and hornblende were separated using standard magnetic techniques on the coarsest grains that were not composite (usually 60–80 mesh). The samples were further purified by meticulous hand-picking, ensuring purity of ~99%.

The $^{40}Ar/^{39}Ar$ measurements on populations of separated grains were conducted in the Radiogenic Isotopes Laboratory at The Ohio State University, Columbus, using general procedures that have been described previously (Foland et al., 1993 and references therein). Aliquots of approximately 80–100 mg for hornblende and 6–10 mg for mica were irradiated in the Ford Nuclear Reactor of the Phoenix Memorial Laboratory at the University of Michigan for ~100 h. Subsequently, the irradiated aliquots were heated incrementally by resistance heating in high-vacuum, low-blank furnaces to successively higher temperatures, with a dwell time of about 40 min at each temperature. These incremental-heating fractions were analyzed by static gas mass analysis with a Nuclide 6-60-SGA mass spectrometer or a MAP 215-50 mass spectrometer, typically in about 12–15 or 25–30 steps, respectively. The analytical results are summarized in Table 2, with all analytical data in Table A3 which provides full experimental details (e.g., isotopic concentrations, K, Ca, and Cl contents, monitor used) plus all the ages for the total-gas (or integrated) and the plateau (if observed) fractions. An overall systematic uncertainty of ±1% is assigned to J values to reflect uncertainty in the absolute age of the monitor. Typically, this uncertainty is not included when age uncertainties are quoted, in order to emphasize the level of apparent age dispersion among plateau fractions, and to allow the comparison of plateaus among samples using a common monitor. The results of the $^{40}Ar/^{39}Ar$ incremental-heating analyses presented as release spectra are available upon request.

In order to further document cooling age gradients preserved within individual minerals, the $^{40}Ar/^{39}Ar$ laser microprobe was utilized on single muscovite crystals. The Ar-laser microprobe analysis is an important method in assessing age gradients within a single crystal and providing additional information unobtainable by conventional $^{40}Ar/^{39}Ar$ methods. Published studies have indicated that conventional, incremental heating of the crystal can homogenize intracrystalline gradients in ^{40}Ar, and may mask important details of the thermal history of analyzed samples (Hodges and Bowring, 1995). Ar-laser spot analysis provides the means necessary to test for gradients within a single crystal; if they exist, large gradients within the crystal represent variations in the composition of ^{40}Ar concentration. The variations may result from selective uptake of "excess" ^{40}Ar, or may be a product of simple diffusion loss at the scale of the physical grain size boundary, along zones of high dislocation density, or by thermal resetting (Kelley and Turner, 1991; Hames and Hodges, 1993). By constructing age-distribution maps of the analyzed grains, a reconstruction of the thermal history of the orogen will be more readily constructed.

$^{40}Ar/^{39}Ar$ laser microprobe analyses were performed at the Massachusetts Institute of Technology, Cambridge, using procedures similar to those described in Hodges and Bowring (1995). Mica grains of a few millimeters in size were selected and irradiated in the C5 position in the McMaster University nuclear reactor for 35 h with a total power of 70 MW. The conversion efficiency of ^{39}K to ^{39}Ar was monitored using Taylor Creek rhyolite with an apparent age of 28.34 Ma (Renne et al., 1998). The values of irradiation parameter J determined from measurement of the monitors were 0.01676–0.01684 with uncertainties less than 0.5%. K_2SO_4 and CaF_2 synthetic salts were used to enable corrections for interfering nuclear reactions.

Samples were ablated with a New Wave excimer (UV) laser in raster mode. The laser size varied from 145 to 235 μm for each sample. Spot analysis was carried out by firing the laser three consecutive times at 900 bursts/s at a repetition rate of 20 Hz. The total heating time of each analysis was 600 s with an accumulation time of 300–600 s. The laser power output fluctuated between 84 and 120 mJ with a slight variation in voltage of ~30 kV. Released gasses were purified for 10–15 min with Al–Zr and Fe–Zr–V getters and then admitted into a MAP 215-50 mass spectrometer for Ar isotopic analysis using an electron multiplier. System blanks were measured before and after each sample, and all data were corrected for blanks and mass-fractionation effects. Final data reduction was conducted with the program ArArCalc (Koppers, 2002). Precision limits represent propagated measurement uncertainties and are reported throughout this paper at the 1σ level. The generally good agreement among individual fusion analyses of a given sample produced standard errors for each sample that are significantly smaller than the 1σ errors on many of the individual analyses. The reported results of these analyses are presented in Table A4 and as "age contour" maps (Fig. 5), in which contour lines represent similar ages within the grain.

Table 2
Summary of $^{40}Ar/^{39}Ar$ analytical results and ages, western Lake Superior

Sample name	Lithology	%K	T_g (Ma)	T_p (Ma)	$\%^{39}Ar$	Run#
Muscovite						
97-CM-7	Pegmatite	6.6	1715	1716 ± 5	96	57C14
94-MI-1	Musc. schist	5.3	1640	1673 ± 6	50	53I3
96-MI-5	Pegmatite	6.5	1647	1653 ± 4	75	53I16
97-CM-10	Pegmatite	6.5	1566	1569 ± 5	95	57C20
97-CM-13	Pegmatite	5.1	1362	1366 ± 6	87	57C27
Biotite						
97-CM-6b	Amphibolite	4.0	1379	N/A		57C12
MON-1	Tonalite	5.5	1344	1358 ± 4	86	58B50
97-CM-11	Granitic gneiss	4.0	1254	1268 ± 5	77	57C23
97-CM-3	Musc.-bio gneiss	4.3	1249	N/A		57C7
PRV-1	Biotite gneiss	7.0	1128	1135 ± 5	86	58B8
WI-7	Biotite gneiss	0.7	1116	1128 ± 3	88	53I28
#80	Tonalite gneiss	3.9	1058	1067 ± 5	91	57C3
#76	Biotite gneiss	8.5	1358	1372 ± 4	55	58B47
WI-4	Quartz monzonite	6.5	1437	1456 ± 4	71	53I25
97-CM-15	Quartz monzonite	4.0	1419	1435 ± 4	92	57C31
BIRON	Amphibolite dike	5.5	1582	1600 ± 5	85	58B38
WRB-PV	WRB granite	5.5	1420	1439 ± 6	82	58B30
“(MAP)		6.1	1408	1428 ± 5	87	58B28M
96-WIS-25	Sheared amphibolite	4.8	1365	1403 ± 5	75	58B19
96-WIS-15	WRB granite	5.2	1445	1464 ± 7	93	58B44
“(MAP)		6.6	1440	1460 ± 5	87	58B43M
WI-95-3	WRB granite	5.3	1365	1415 ± 4	72	58B41
96-WIS-26	WRB granite	5.7	1405	1426 ± 4	75	58B27
96-WIS-17	WRB granite	5.6	1416	1427 ± 4	76	58B13
Hornblende						
96-MI-4	Amphibolite	0.6	1797	1799 ± 6	91	53I14
97-CM-4	Amphibolite	0.7	1717	1765 ± 8	86	57C9
“(MAP)		0.8	1730	1770 ± 6	63	57C8M
97-CM-9	Amphibolite	0.6	1769	1785 ± 8	83	57C18
“(MAP)		0.6	1776	1789 ± 5	89	57C17M
97-CM-8	Amphibolite dike	0.8	1628	1646 ± 6	71	57C16
97-CM-12	Amphibolite	0.4	1624	“1640 ± 6”	52	57C25
97-CM-14a	Amphibolite	0.8	1489	1514 ± 9	65	57C29
DS-96-7	Amphibolite	0.1	1380	“1568 ± 12”	26	58B16
“(MAP)		0.1	1388	1664 ± 15	25	58B15M
WI-97-1	Amphibolite	0.3	1390	1432 ± 8	77	58B33
“(MAP)		0.3	1389	“1439 ± 4”	72	58B31M
WI-95-3 (MAP)	WRB granite	0.6	1404	N/A		60B30M
“(MAP)		0.7	1419	1422 ± 2	64	60B31M
97-DR-23	Banded gneiss	0.6	1473	“1514 ± 5”	57	57A21
96-DR-13	Hornblende schist	0.4	1421	“1438 ± 6”	76	58B24
“(MAP)		0.4	1409	1434 ± 5	84	58B23M

%K: the approximate K concentration of sample in weight %, derived from ^{39}Ar yields; T_g: the total-gas age derived from the summation of all fractions of the incremental-heating analysis; T_p: the plateau age derived from the incremental-heating age spectrum. For those in quotation, the dispersion among the included fractions exceeds variations from analytical uncertainties. MAP samples re-analyzed on MAP 215-50 mass spectrometer line.

5. Metamorphic geochronometry results

Coupled with results from our previous metamorphic geochronology study, sample locations cluster in three main regions (Fig. 2): the eastern orogen that encompasses the two main metamorphic regions in Michigan, the central orogen east of the midcontinent rift in Wisconsin, and the western orogen, west of the rift, which surrounds the 1775 Ma east-central Minnesota batholith.

5.1. Eastern orogen

Sample MI-ST, a fine-grained metapelitic biotite schist containing large garnet and staurolite porphyroblasts in a predominantly mica and quartz matrix, was sampled from the Republic metamorphic node in Marquette County, Michigan. The well defined staurolite range in size from <1 mm up to 4 mm in length, while the garnet occurs as euhedral grains of approximately 1 mm in length. Monazite grains within the sample range from approximately 5 to 50 μm in length. Unfortunately, no monazites were identified as mineral inclusions; the monazite grains analyzed were located along the biotite–quartz boundaries within the planes of foliation. In total, 30 spots on 12 grains from MIST were analyzed *in situ* via the ion microprobe and yielded a mean $^{207}Pb/^{206}Pb$ age of 1758 ± 5 Ma (MSWD = 1.1; Table 1).

To determine the presence of age domains smaller than the resolution of the ion microprobe sputter diameter, a subsequent analysis of sample MI-ST was conducted utilizing the EMPA technique. There were 13 monazite grains identified in thin section, which appear to be relatively homogeneous with respect to elemental concentrations, and two grains have a skeletal appearance. A total of 23 spots on 6 grains yielded a mean age of 1768 ± 13 Ma (MSWD = 9.0). Five individual spot analyses indicate a potential age domain at 1830 Ma. Notably, the results of the EMPA technique yielded results concordant with those obtained via the ion microprobe method.

An Archean basement gneiss, sample CREP, was collected within the sillimanite zone of the Republic metamorphic node, south of the Republic synform in Marquette County, Michigan. The sample is a pink to gray coarse-grained foliated gneiss containing quartz, microcline, Na-plagioclase, and biotite. Monazite grains generally occur along quartzofeldspathic boundaries, and range from 60 to 150 μm in length. The majority of the monazite identified in thin section was skeletal and heterogeneous, containing inclusions of apatite and thorite. A total of 14 spots on 4 separate grains were performed on this sample, yielding two separate $^{207}Pb/^{206}Pb$ age domains: 2576 ± 18 Ma (MSWD = 16) and 2116 ± 83 Ma (MSWD = 4.0). The percentages of radiogenic ^{208}Pb and ^{206}Pb were as low as 70% (Table A1), while Th/U ratios ranged from 23 to 169, suggesting that this sample was relatively chemically heterogeneous (and altered) and had a high concentration of ^{204}Pb such that these dates should actually be slightly younger. With such large errors and minimal radiogenic Pb signals, the EMPA method was also applied to sample CREP to elucidate smaller and/or younger age domains and remedy inconsistencies with this sample.

Three out of four grains of sample CREP analyzed by the ion microprobe method were also analyzed by the *in situ* EMPA technique, including one additional monazite grain approximately 60 μm in length. Elemental concentration maps indicate the heterogeneity of these grains with respect to Y, Th, Ca, and U (Rose, 2004), and areas with extreme concentrations of these elements were avoided during analyses. The objective was to specifically target younger age domains within a single grain. In total, 78 spots on these four grains yielded a range of total-Pb mean ages, but two significant age domains at 2577 ± 19 Ma (MSWD = 12) and 1780 ± 14 Ma (MSWD = 7.0). The powerful combination of ion microprobe and EMPA analyses confirm the presence of two significant age domains at ca. 2600 and 1780 Ma (Fig. 3 and Table 1).

Within the Peavy metamorphic node south of Republic, one sample was collected for geochronometric analyses. Sample PVD is a medium to fine-grained micaceous schist, located within the kyanite zone of the node near the Peavy Dam about 24 km west of Foster City, Michigan in Dickinson County. Monazite grains found within the sample ranged from approximately 10 to 60 μm in length and were primarily located along the boundaries of biotite and quartz grains within the matrix. Although some of the monazite grains exhibit a skeletal appearance, the majority display a more pristine appearance compared to most other samples in this study. Collectively, 14 spots on 7 grains were analyzed *in situ* via the ion microprobe and yielded a mean $^{207}Pb/^{206}Pb$ age of 1828 ± 7 Ma (MSWD = 2.5).

Sample HRR, a fine- to medium-grained gneiss containing quartz, biotite, amphibole, and muscovite, was collected near Peavy Pond in Copper County, Michigan. Seven monazite grains were identified in thin section ranging in size from 20 to 30 μm in diameter. In total, 19 EMPA spots on 5 grains were analyzed, and produced a combined mean total-Pb age of 1765 ± 28 Ma (MSWD = 30). More significantly, one domain of a subset of 10 spot analyses was identified with an age of 1774 ± 7 Ma (MSWD = 1.4; Table 1).

5.2. Central orogen

Sample 96-17 was collected near the eastern shore of Blockhouse Lake in the Park Falls metamorphic terrane, approximately 8 km east of Park Falls, Wisconsin in Price County. This sample is a fine- to medium-grained biotite schist containing potassium feldspar, muscovite, and quartz within the matrix. Monazite located in

the sample predominantly occurs along biotite–quartz boundaries in the foliation planes. Overall, monazite grains analyzed from this sample are elementally homogeneous and range in size from 40 to 100 μm in length. In total, 15 ion microprobe spot analysis on 7 monazite yielded a mean $^{207}Pb/^{206}Pb$ age of 1799 ± 3 Ma (MSWD = 1.6; Table 1).

Away from the internides of the orogen, a coarse-grained garnet staurolite schist, sample HS-4, was collected near Hamburg, Wisconsin in the central Wisconsin magmatic terrane (Fig. 2). A total of 41 spots on seven monazite grains were analyzed of which 6 were discarded due to instrument variation. The $^{207}Pb/^{206}Pb$ ages range from approximately 1780 to 1700 Ma and the relative probability graph shows a single peak at 1744 ± 3 Ma (MSWD: 0.7). This age is 20–30 million years younger than the other geon 17 dates in the region, and also the sample which is farthest south.

5.3. Western orogen

To supplement the monazite ages from two samples presented in Schneider et al. (2004), five samples were dated from the western Penokean orogen (Fig. 2): one sample via ion microprobe and four via EMPA (Fig. 3 and Table 1). Sample AM-016 is a well-foliated, medium-grained, staurolite–biotite schist collected north of County Route 2 east-northeast of the town of Malmo, Minnesota. This sample contains predominantly elongate monazite grains displaying a mottled chemical variation in Y and Th content. Six grains were analyzed and one was contained within staurolite while the remaining were within the matrix. The analyses yielded a mean total-Pb age of 1741 ± 4 Ma (MSWD: 2.1).

Sample MN-29 is a coarse-grained staurolite schist from the Little Falls Formation collected at the base of Blanchard Dam on the Mississippi River (Morrison County). The staurolites are 3–4 cm euhedral crystals and crosscut the fabric and in some crystals preserve the overall fabric of the unit. The rocks also contain anhedral pinhead garnets that have inclusion-rich cores and relatively infusion-free rims. These garnets occur within the matrix and as inclusions within the staurolite. Foliations consist of biotite-rich layers that alternate with quartz and plagioclase-rich layers. Elemental analysis of this sample yielded a mean total-Pb age of 1759 ± 6 Ma (MSWD: 7.9) from a subset of 92 spots on five grains.

Also from the Little Falls Formation ~25 km southwest of sample MN-29, sample P-16 is a coarse-grained staurolite schist, provided by the Minnesota Department of Natural Resources as a drill core. The rock has similar mineralogy and textures to sample MN-29 described above and Holm and Lux (1996) obtained a 1755 Ma $^{40}Ar/^{39}Ar$ biotite plateau age from this sample. The sample contains monazite with very irregular grain boundaries, numerous inclusions, and variable Th content. Schneider et al. (2004) presented 24 preliminary spot total-Pb dates from this sample, and in addition to the 115 spot analyses on seven new grains presented here, analyses yield a mean total-Pb age of 1776 ± 4 Ma (MSWD: 5.0).

Sample PO-23 is a slightly foliated coarse-grained staurolite-garnet schist collected at an abandoned railroad cut near the town of Denham, Pine County, Minnesota. The staurolite in the rock are up to 1–2 cm in length and the monazite are relatively euhedral with irregular grain boundaries and very few inclusions; all monazite analyzed in this sample were contained within the mica–quartz matrix. Seven grains were analyzed with 85 spots, yielding two prominent age populations: 1844 ± 7 Ma (MSWD: 2.5) and 1788 ± 4 Ma (MSWD: 2.4).

A sample of the Sartell Gneiss, sample S-2, is a well-foliated, dark-brownish-gray biotite gneiss that is interlayered on a cm-scale with somewhat coarser-grained, granular quartzofeldspathic gneiss. Much of the gneiss exhibits layering and foliation that are folded about an east-trending axis. Mafic enclaves within the Sartell Gneiss have textures and mineral assemblages that are unequivocally igneous (Dacre et al., 1984). Sample S-2 was collected west of U.S. Highway 10 northeast of the town of Sartell (Fig. 2). Holm et al. (1998a) obtained a $^{40}Ar/^{39}Ar$ biotite plateau age of 1751 ± 11 Ma and our EMPA total-Pb analysis on this sample yielded a mean age of 1756 ± 5 Ma (MSWD: 5.9) after 102 spot analyses. This sample was also dated via ion microprobe analyses. Through SEM imaging prior to analyses, rim textures were found to be spatially distinct from core and minor interior replacement textures; rims and replacement textures are characterized by high-Th content and spatially defined as mineralogically discordant growth sectors. However, in all cases age data are indistinguishable between domains and replacement probably resulted from the same thermal event as the rim growth. Isotopic analysis yielded a mean $^{207}Pb/^{206}Pb$ age of 1777 ± 3 Ma (MSWD = 0.5) and is comparable to the 1760 Ma total-Pb age (Table 1).

6. $^{40}Ar/^{39}Ar$ thermochronometry results

Table 2 summarizes the results of eleven new hornblende ages, five new muscovite ages, and 15 new biotite ages from the central and eastern orogen. The loca-

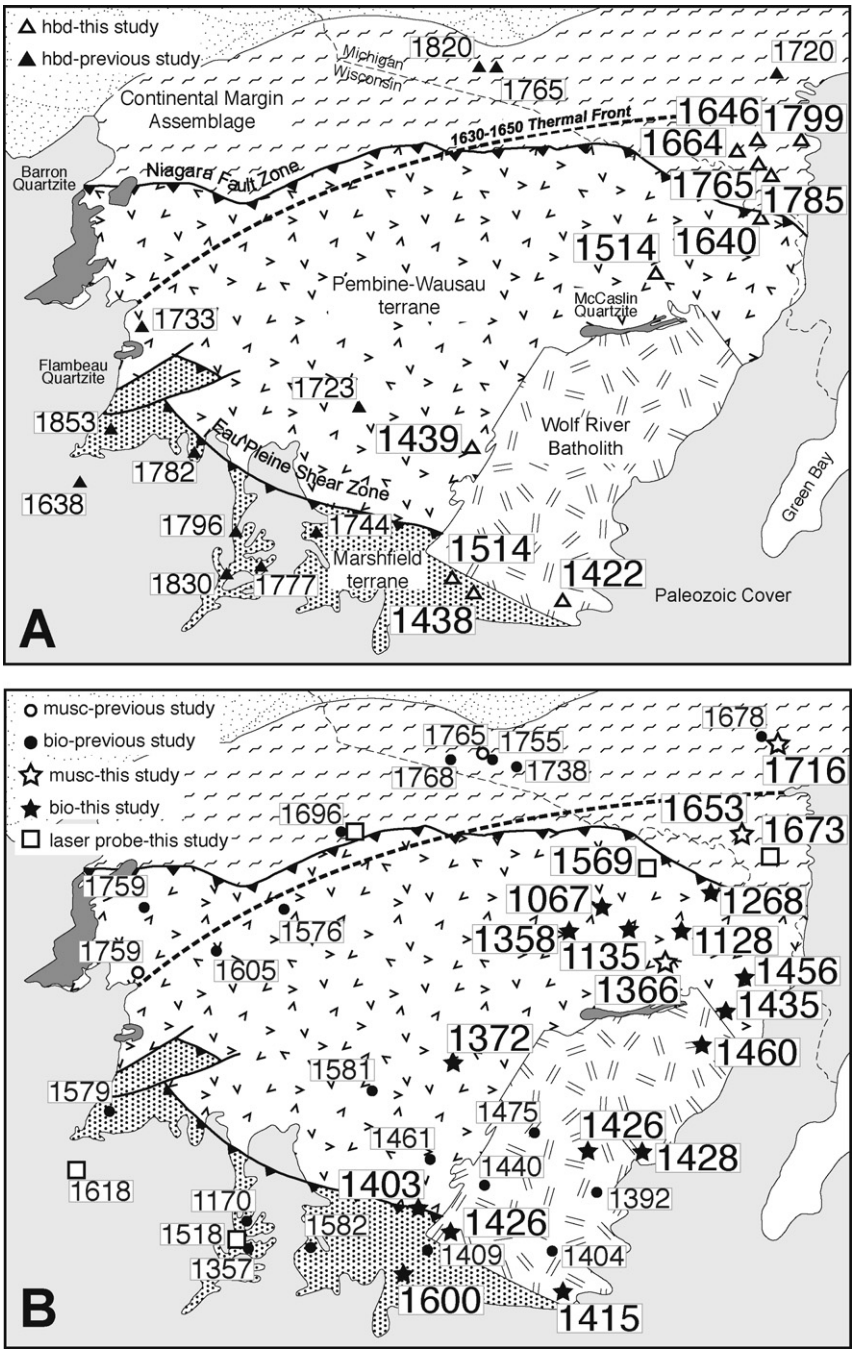

Fig. 4. Generalized geologic map of the central and eastern orogen (same lithologic patterns as Fig. 2; Baraboo Interval quartzites are dark gray). Location and (A) hornblende and (B) mica $^{40}Ar/^{39}Ar$ cooling ages from this study and previous studies (Schneider et al., 1996; Romano et al., 2000). Larger text boxes are results from this study. The "1630–1650 Ma thermal front" represents a break in mica cooling ages and corresponds to a deformational front in the overlying quartzites in northwest Wisconsin (Holm et al., 1998b).

tions and plateau ages are plotted in Fig. 4 together with published $^{40}Ar/^{39}Ar$ ages and locations from Schneider et al. (1996) and Romano et al. (2000) for regional comparison. Seven single muscovite grains were also dated via laser probe methodology; results of spot ages are illustrated in Fig. 5 and reported below in the context of the conventional mica cooling age results.

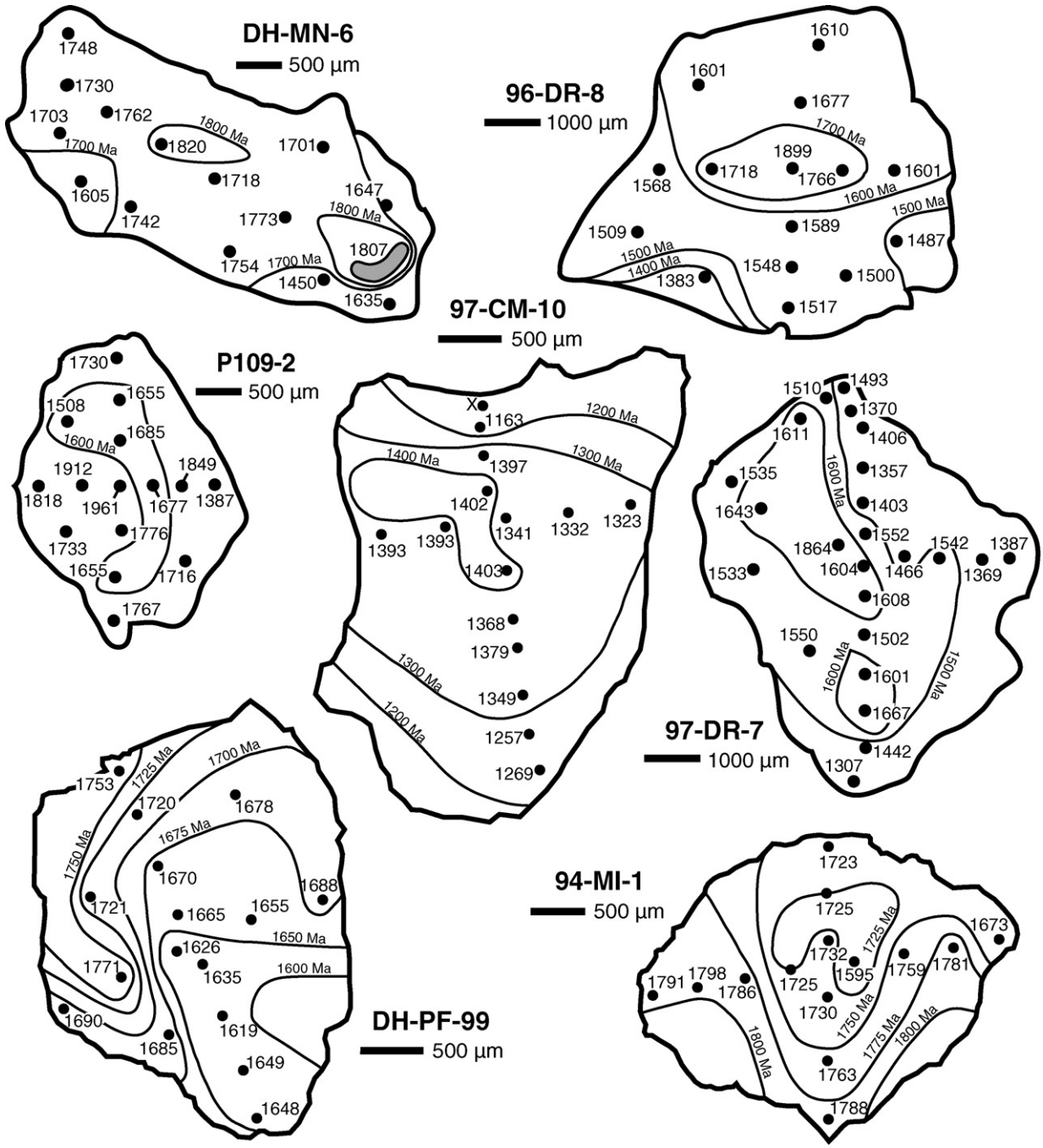

Fig. 5. Muscovite age contour maps of $^{40}Ar/^{39}Ar$ laser microprobe analyses. Each solid circle represents ablated location with corresponding isotopic age (in Ma). Contour lines were interpolated between points through a somewhat subjective process. Isotopic data available in Table A4.

6.1. Hornblende cooling ages

The hornblende data yield excellent results with almost all separates giving reliable plateau or near-plateau ages. Five ages from northern Michigan north of the Niagara fault zone and one from northern Wisconsin just south of the fault fall into two separate clusters: an older population in the 1799–1765 Ma range and a younger population in the 1664–1640 Ma range (Fig. 4A). The early geon 17 hornblende ages are concordant with the youngest metamorphic monazite ages from the northern orogen in Michigan and with the major-

ity of hornblende $^{40}Ar/^{39}Ar$ ages obtained from bedrock Precambrian samples in the western orogen in western Wisconsin and east-central Minnesota.

Four hornblende cooling ages were also obtained from country rock adjacent to the Wolf River batholith (Fig. 4A). All four samples yield geon 14 or late geon 15 plateau or near-plateau ages. These are the youngest hornblende ages reported across the entire southern Lake Superior region, clearly showing the thermal effects of the Wolf River plutonism upon the adjacent country rock. One igneous hornblende sample from a distinct phase of the batholith yielded a reliable plateau age of 1422 ± 2 Ma.

6.2. Mica cooling ages

Twenty new $^{40}Ar/^{39}Ar$ incremental-heating mica cooling ages from the central and eastern orogen range from as old as 1716 Ma in the north to as young as 1067 Ma in the juvenile magmatic terrane (Fig. 4B). The majority of samples yield excellent results with most producing reliable $^{40}Ar/^{39}Ar$ plateau or near-plateau ages (Table 2). In addition, the results of spot laser microprobe analyses on seven coarse grains of muscovite are shown schematically in Fig. 5 and the analytical results given in Table A4. The results are discussed below, with the samples being separated geographically into two groups based on the location north and south of the geon 16 Mazatzal-interval thermal front (Holm et al., 1998b).

6.2.1. North of the Mazatzal thermal front

The northernmost conventionally dated basement muscovite sample yielded a 1716 ± 5 Ma $^{40}Ar/^{39}Ar$ plateau age which is only slightly younger than hornblende cooling ages from this region (Schneider et al., 1996; Tohver et al., 2007).

Muscovite DH-MN-6 was collected from the Neoarchean McGrath Gneiss in east-central Minnesota. This sample was picked from a coarse-grained, pinkish-gray biotite–muscovite gneiss commonly containing megacrysts of microcline (Holm et al., 1993); Holm and Lux (1996) obtained an $^{40}Ar/^{39}Ar$ muscovite plateau age of 1705 ± 19 Ma. Of the 15 laser spots, cooling ages range from 1820 to 1605 Ma and yield a total fusion age of 1701 ± 3 Ma, with the exception of a 1450 Ma rim age (Fig. 5). Generally, the oldest ages are distributed within the center of the grain and young outward toward the edge of the grain.

A sample was also collected just north of the McGrath Gneiss sample: muscovite P109-2 is from an amphibolite facies, coarse-grained staurolite–biotite schist. Fifteen spot analyses yielded ages ranging between 1961 and 1655 Ma, with the exception of a single geon 13 age and a single geon 15 age (Fig. 5). The $^{40}Ar/^{39}Ar$ total fusion age for this sample is 1738 ± 2 Ma, and the age pattern that emerges illustrates a reversely age-zoned crystal, with primarily younger cooling ages distributed in the center.

Muscovite DH-PF-99 is a ~2.5 mm muscovite grain from a 1781 Ma two-mica granite located just south of the town of Park Falls, northern Wisconsin (Holm et al., 2005). Sixteen laser spots obtained on two main perpendicular traverses yielded a 150 million years cooling age gradient, ranging from 1753 to 1619 Ma. The age contour map shows a distinct lack of concentricity possibly related to grain breakage.

6.2.2. South of the Mazatzal thermal front

Three muscovite separates from basement units of the east-central orogen yielded $^{40}Ar/^{39}Ar$ plateau ages of 1673, 1653, and 1569 Ma (Table 2). These cooling ages are substantially younger than the >1765 Ma cluster of hornblende cooling ages described above, but are roughly concordant with the younger cooling age cluster. An anomalously young muscovite plateau age of 1366 Ma was obtained from a locality north of the Wolf River batholith (Fig. 4B).

Muscovite 97-DR-7 was obtained from an Archean muscovite-rich granite located ca. 10 km west of Neillsville, west-central Wisconsin. Romano et al. (2000) obtained a $^{40}Ar/^{39}Ar$ total-gas age of 1518 Ma and a highly discordant spectrum; the authors attributed no geological significance to the 1518 Ma age. In this study, 24 laser spots were analyzed along a single transect with additional spot analyses along the edges. With the exception of one 1864 Ma core age, the $^{40}Ar/^{39}Ar$ ages range from 1667 to 1307 Ma, yielding a total fusion age for this sample of 1545 ± 4 Ma. The 350 million years age gradient has a pseudo-concentric pattern (Fig. 5).

A pegmatite dike in the town of Little Falls on the north side of the Eau Claire River, Wisconsin was collected for muscovite sample 96-DR-8. Romano et al. (2000) obtained a $^{40}Ar/^{39}Ar$ plateau age of 1614 ± 5 Ma. Fifteen laser spot ages on one grain reveal a 500 million years age gradient with the oldest ages concentrated within the center of the crystal and younger ages toward the edges of the grain. With the exception of the 1899 Ma core age, cooling ages range between 1766 and 1383 Ma; the $^{40}Ar/^{39}Ar$ total fusion age for this sample is 1592 ± 7 Ma.

Muscovite grain 94-MI-1, from an Archean biotite–muscovite schist, was collected near Foster City,

northern Michigan. This sample yielded a $^{40}Ar/^{39}Ar$ muscovite plateau age of 1673 ± 6 Ma (this study) and U–Pb monazite domain ages of 1832 and 1812 Ma (Schneider et al., 2004). Thirteen laser ablation spots produced a crude reverse-age gradient of ca. 60 million years from ca. 1730 Ma core to ca. 1790 Ma rim (Fig. 5). With the exception of an anomalously young 1595 Ma core age, the grain exhibits an overall concentric pattern with older cooling ages occurring along the rim and younging toward the core.

Coarse muscovite from a Pine River pegmatite body (sample 97-CM-10) was collected south of the Niagara fault zone in northeast Wisconsin. This sample yielded a conventional $^{40}Ar/^{39}Ar$ plateau age of 1569 ± 5 Ma (this study). However, laser microprobe ages are significantly younger: 14 spots revealed an approximate 150 million years age gradient with cooling ages concentrically ranging from 1403 to 1257 Ma with one anomalous outlier at 1163 Ma.

Several biotite mineral separates from south of the thermal front were dated to supplement the muscovite cooling ages (Table 2). One biotite separate collected from the Archean Marshfield terrane exposure at Biron Dam south of the Wolf River batholith yielded a near-plateau age of 1600 ± 5 Ma. In spite of proximity to the intrusion, this age is similar to that of biotite $^{40}Ar/^{39}Ar$ ages reported from bedrock samples in the central orogen. Other biotite cooling ages collected from country rock around the Wolf River intrusion range from 1456 Ma (north of the batholith) to 1372 Ma (west of the batholith). New biotite cooling ages from the intrusion itself range from 1460 Ma (north) to 1415 Ma (south), a range similar to that reported by Holm and Lux (1998). The youngest biotite mineral ages obtained in this study come from Penokean-interval juvenile magmatic arc rocks due north of the northernmost exposure of the batholith (Fig. 4B). Five biotite $^{40}Ar/^{39}Ar$ plateau ages are 1358, 1265, 1135, 1128, and 1067 Ma, the oldest biotite age being concordant with the youngest muscovite cooling age discussed above.

7. Discussion and implications

Determining the timing, extent, and controls of polyphase metamorphism is critical for understanding crustal growth and evolution (Geiger and Guidotti, 1989). This is perhaps especially true for poorly exposed terranes such as the northern U.S. continental interior where metamorphic isograds are difficult to map and correlate between localities. Our study presents the results of complementary techniques used to evaluate the timing of thermal evolution along the southern margin of Proterozoic Laurentia. New metamorphic monazite geochronology presented here, together with other recently published geochronologic data across the west, central and eastern orogen, provide direct age constraints on successions of amphibolite facies metamorphic episodes associated with peak Penokean orogenesis and with subsequent Yavapai orogenesis and its concomitant magmatism. Notably, monazite age data obtained from ion microprobe isotopic analyses compare well with, and in most cases are concordant with, electron microprobe elemental analyses, indicating the robustness of our geochronometric protocol. $^{40}Ar/^{39}Ar$ mineral cooling ages and muscovite laser microprobe ages record the details of variable crustal reheating and cooling following initial Penokean-interval collision. The majority of incremental heating experiments yield well-defined plateau or near-plateau ages, consistent with the overall excellent behavior of $^{40}Ar/^{39}Ar$ systematics found in earlier studies (Holm and Lux, 1996; Schneider et al., 1996; Holm et al., 1998a). In spite of this, the new laser microprobe analyses illustrate that conventional mica thermochronology in this region (Fig. 4B) does not effectively reveal the internal distribution of radiogenic argon within individual crystals. However, the conventional $^{40}Ar/^{39}Ar$ plateau cooling ages do appear to consistently reveal broad, first-order thermal overprinting effects. Our results show that $^{40}Ar/^{39}Ar$ laser microprobe analyses can be an effective, complementary tool for revealing higher-order details of the complex thermal histories that exist in polymetamorphosed Precambrian terranes. Only by considering the results from all three areas collectively can we gain a complete understanding of the evolution of juvenile crust in the continental interior.

7.1. Western orogen

Overall, the dominant amphibolite facies metamorphic signature in the deepest regions of the orogen (north of the main suture) occurred between 1800 and 1750 Ma, well after Penokean-interval convergence ended. Perhaps not surprisingly, monazite crystallization age data indicate that the most extensive geon 17 amphibolite facies conditions occurred adjacent to the 1775 Ma East-central Minnesota batholith; here in the western orogen Penokean-interval amphibolite facies metamorphism is preserved only within the fold-and-thrust belt north of the McGrath gneiss dome. This metamorphic-age transition is marked by the Malmo structural discontinuity which juxtaposes post-Penokean plutons in the hanging wall against slightly lower grade rocks of the medial

zone in the footwall to the north. These observations are consistent with the Malmo discontinuity being a geon 17, possibly reactivated Penokean-interval, structure that elevated the plutonic-gneiss dome terrane of east-central Minnesota relative to lower grade rocks in a manner similar to that recently proposed for extrusion of the gneiss dome corridor in the central and eastern orogen (see Fig. 9 of Schneider et al., 2004).

Rapid cooling of the metamorphic terrane in east-central Minnesota following geon 17 metamorphism was associated with differential exhumation and followed by deposition of supermature siliciclastic rocks of the Baraboo Interval (i.e., Sioux quartzite). Because the sub-Paleoproterozoic nonconformity approximates the current erosional surface in Minnesota and Wisconsin (i.e., Barron quartzite), these basement rocks have not been significantly buried since they were exhumed over 1700 million years ago. In spite of this history, muscovite grains from this region all reveal significant cooling age gradients of >100 million years. We interpret the geon 16 Mazatzal-interval spot ages to indicate mild reheating—possibly associated with fluid flow outboard of the Mazatzal tectonic front. Fluid expulsion in front of deformed foreland regions is not uncommon, and may have also occurred throughout the eastern orogen near the Republic gneiss dome where geon 16 Rb/Sr ages are also abundant (Van Schmus and Woolsey, 1975). In support of this interpretation, Hanley et al. (2006) obtained a ~1615 Ma Ar/Ar age on detrital muscovite from the base of the Sioux quartzite suggesting limited isotopic resetting due to Mazatzal age fluid migration.

7.2. Eastern orogen

The metamorphic nodes of northern Michigan, though relatively simple in map view, formed during multiple tectonothermal events. Schneider et al. (2004) documented peak Penokean metamorphism in Archean gneiss from the Peavy node area. However, our new results here indicate that an early geon 17 amphibolite facies metamorphism also affected this region, even though it lacks any (exposed) evidence for geon 17 magmatism. A post-Penokean-interval ca. 1800 Ma pluton in the central part of the Republic node appears to have imposed an initial weak metamorphic imprint (Tohver et al., 2007). However, the dominant amphibolite facies metamorphism is 1780–1760 Ma and likely related to gneiss dome genesis (Tinkham and Marshak, 2004; Schneider et al., 2004).

The eastward extent of the Mazatzal deformational front in this region is not well determined because the area lacks the Baraboo Interval quartzites which serve as excellent strain markers for geon 16 deformation. Assuming mica $^{40}Ar/^{39}Ar$ systematics closely approximate the deformational front as is the case in the central orogen (Fig. 4B), our new basement $^{40}Ar/^{39}Ar$ cooling age data (especially muscovite) suggest that the Mazatzal tectonic front is located between the concentric Republic node and the east-west elliptical Peavy node to the south (Holm et al., 1998b). In the Republic area, muscovite $^{40}Ar/^{39}Ar$ cooling ages are concordant with hornblende cooling ages, whereas Rb/Sr biotite dates are completely reset to ca. 1630 Ma. Resetting of Rb/Sr biotite ages, but not $^{40}Ar/^{39}Ar$ ages, reflects Rb greater susceptibility to lower-temperature mobility. We suggest that the Republic area escaped significant Mazatzal-interval deformation, but did undergo some lower-temperature, possibly hydrothermal, metamorphism at 1650–1630 Ma.

Around the Peavy metamorphic node, muscovite $^{40}Ar/^{39}Ar$ dates are nearly completely reset at 1650 Ma and are substantially younger than some of the hornblende cooling ages. In addition, three of the hornblende $^{40}Ar/^{39}Ar$ ages are completely reset at ca. 1650 Ma, indicating localized moderate-temperature reheating perhaps also caused by fluid-related activity or dynamic recrystallization. South-directed basement thrusts mapped in the Peavy region, previously interpreted as Penokean-interval backthrusts, may actually be features which accommodated substantial Mazatzal-interval foreland shortening. The implication of this interpretation is that the Mazatzal foreland deformation mode in the southern Lake Superior region was not simply thin-skinned.

7.3. Central orogen

Kyanite- and sillimanite-bearing rocks of the continental margin in northern Wisconsin were metamorphosed at 1830 Ma, 1800 Ma, and ca. 1765 Ma, all associated with known pulses of magmatic activity across the region (Schneider et al., 2004; Holm et al., 2005). Our new metamorphic monazite Pb/Pb age of 1799 ± 3 Ma (sample 96-17) from near Park Falls, Wisconsin confirms the intermediate-age metamorphic event.

Metamorphic grade of the Wisconsin magmatic terrane rocks overall south of the Niagara fault zone is upper greenschist to locally lower amphibolite facies. In the central orogen, Romano et al. (2000) reported two hornblende $^{40}Ar/^{39}Ar$ cooling ages that were likely a result of Penokean-interval metamorphism (1853 and 1830 Ma) and several others that were substantially younger (between 1796 and 1723 Ma; Fig. 4A). They

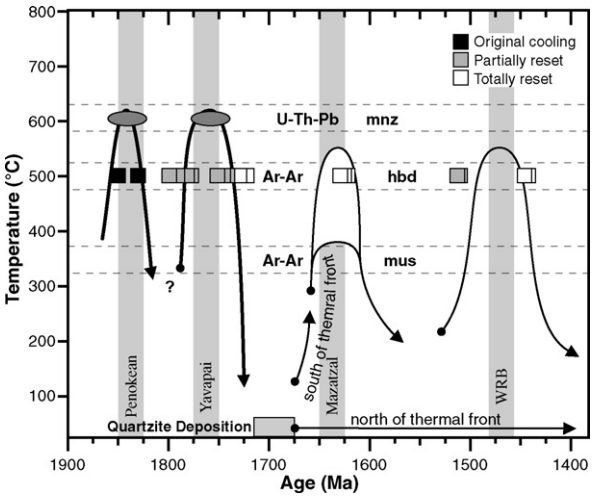

Fig. 6. Temperature–time diagram from the Paleo- and Mesoproterozoic basement of the western Lake Superior region. Evolution path constructed primarily from recent U–Th–Pb monazite and $^{40}Ar/^{39}Ar$ hornblende and mica data (this study; Schneider et al., 2004; Romano et al., 2000). Vertical gray bars represent noteworthy intervals of convergence or magmatism in the region (WRB: Wolf River batholith). Note the divergence of cooling histories (between the north and south) shortly following Baraboo Interval quartzite deposition.

attributed the geon 17 cooling ages to partial resetting of Penokean-interval metamorphic dates during Mazatzal deformation (see proposed *T–t* reconstruction, Fig. 5 of Romano et al., 2000). Our new metamorphic monazite Pb/Pb age of 1744 ± 3 Ma from the garnet–staurolite bearing Hamburg Schist (sample HS) allows for an alternative interpretation. We propose that the abundance of geon 17 hornblende cooling ages preserved in the central orogen reflects a discrete post-Penokean-interval moderate to low grade thermal event that occurred prior to Mazatzal deformation and reheating. We suggest that metamorphism related to accretion of a Yavapai-interval arc was responsible for total to partial resetting of hornblende $^{40}Ar/^{39}Ar$ ages (Fig. 6). Unlike the relatively high grade geon 17 metamorphism documented near the East-central Minnesota batholith, geon 17 metamorphism in the central orogen was only upper greenschist facies and, thus, responsible for only partial resetting of hornblende $^{40}Ar/^{39}Ar$ ages over a significant area. Nevertheless, the gap in hornblende cooling ages between 1725 and 1630 Ma (Fig. 6) suggests that the thermal effects of Yavapai-interval metamorphism were greater than subsequent metamorphism during Mazatzal deformation, which caused hornblende age resetting only locally in the eastern orogen.

Portions of southernmost Wisconsin and much of Iowa experienced amphibolite facies metamorphism commonly attributed to geon 14/15 anorogenic magmatism. New Ar/Ar hornblende ages from drill core samples (Van Schmus et al., 2007) and monazite geochronology from metamorphosed pelitic units of the Waterloo quartzite in southcentral Wisconsin (Stonier, 2006) provide evidence that amphibolite metamorphism is geon 16 and related to Mazatzal-interval accretion.

7.4. Mesoproterozoic events

The youngest hornblende $^{40}Ar/^{39}Ar$ cooling ages from localities immediately adjacent to the Wolf River batholith (Fig. 4A) clearly delineate a zone of complete to nearly complete resetting above ca. 500 °C. Similarly, a relatively narrow zone of reset biotite cooling ages also exists in country rock surrounding the batholith (Fig. 4B). Cooling from geon 14 contact metamorphism is depicted in our revised time–temperature plot for the region (Fig. 6). For the most part, country rock biotite cooling ages are concordant to nearby granite biotite cooling ages. The northern part of the batholith yields the oldest cooling ages possibly indicating that this portion of the batholith intruded at the shallowest crustal levels (Holm and Lux, 1998).

Significant $^{40}Ar/^{39}Ar$ cooling age gradients are also preserved in three muscovite grains south of the Mazatzal tectonic front. Not surprisingly, these micas reveal significant portions of Mazatzal-interval ages superimposed on remnant geon 17 (core) ages and variably overprinted by thermal effects of the Wolf River batholith. With the exception of pegmatite sample 97-CM-10, we note that the conventional $^{40}Ar/^{39}Ar$ plateau age, where available, is similar to the weighted mean of the spot fusion age of each sample.

The youngest mica cooling ages reported in this study are all from a region within the Wisconsin magmatic terrane north of the Wolf River batholith (Fig. 4B). Three of the biotite ages are ca. 1100 Ma and clearly suggest thermal reheating related to Midcontinent Rift activity. A significantly larger area of <1200 Ma Rb/Sr biotite dates has been reported from this same area (Peterman and Sims, 1988) and interpreted as an uplifted flexural bulge (called the Goodman Swell) created by rapid loading along the rift axis to the north. In contrast, our mica $^{40}Ar/^{39}Ar$ ages define a much smaller region of <1200 Ma dates. Because much of the 1470 Ma Wolf River batholith intruded into shallow crust and cooled rapidly through 300 °C, it seems likely that the surrounding Precambrian country rock to the north was also shallow and already cooler than 300 °C by 1470 Ma. Given the unlikelihood of 5–10 km of flexural uplift related erosion and cooling (Coakley and Wang, 1992), we propose that the <1200 Ma dates for both systems

reflect shallow intrusion reheating and isotopic resetting. Midcontinent Rift dike swarms exist at the surface in northern Michigan and in central Wisconsin (Green et al., 1987; King, 1990). Schneider et al. (1996) reported 1100 Ma disturbances of $^{40}Ar/^{39}Ar$ spectra in the eastern orogen and Romano et al. (2000) obtained an isolated 1170 Ma $^{40}Ar/^{39}Ar$ biotite date from the central orogen that they also interpreted to be related to rift reheating.

8. Conclusions

Our new metamorphic and cooling age data from the southern Lake Superior region record thermal events over a 700 million years interval, with significant episodes generally becoming progressively younger and more localized to the south (Fig. 6). In the north, geon 18 Penokean-interval amphibolite facies metamorphism is overprinted by geon 17 Yavapai-interval amphibolite facies metamorphism that caused widespread monazite growth and full- to partial-resetting of hornblende $^{40}Ar/^{39}Ar$ ages. In the southern orogen, regional Yavapai and Mazatzal-interval greenschist facies metamorphism is locally overprinted near the Wolf River batholith by geon 14 amphibolite facies metamorphism.

Application of modern geochronologic techniques on Proterozoic rocks of the southern Lake Superior region has also revealed the timing and importance of meta-plutonic events superimposed on the 1850 Ma Penokean orogen. The orogenic belt has been intruded by two batholiths: the ca. 1775 Ma East-central Minnesota batholith and the 1470 Ma Wolf River batholith. Results of our study reveal the dramatically different thermal influence these two intrusions had on the surrounding country rock. The East-central Minnesota batholith

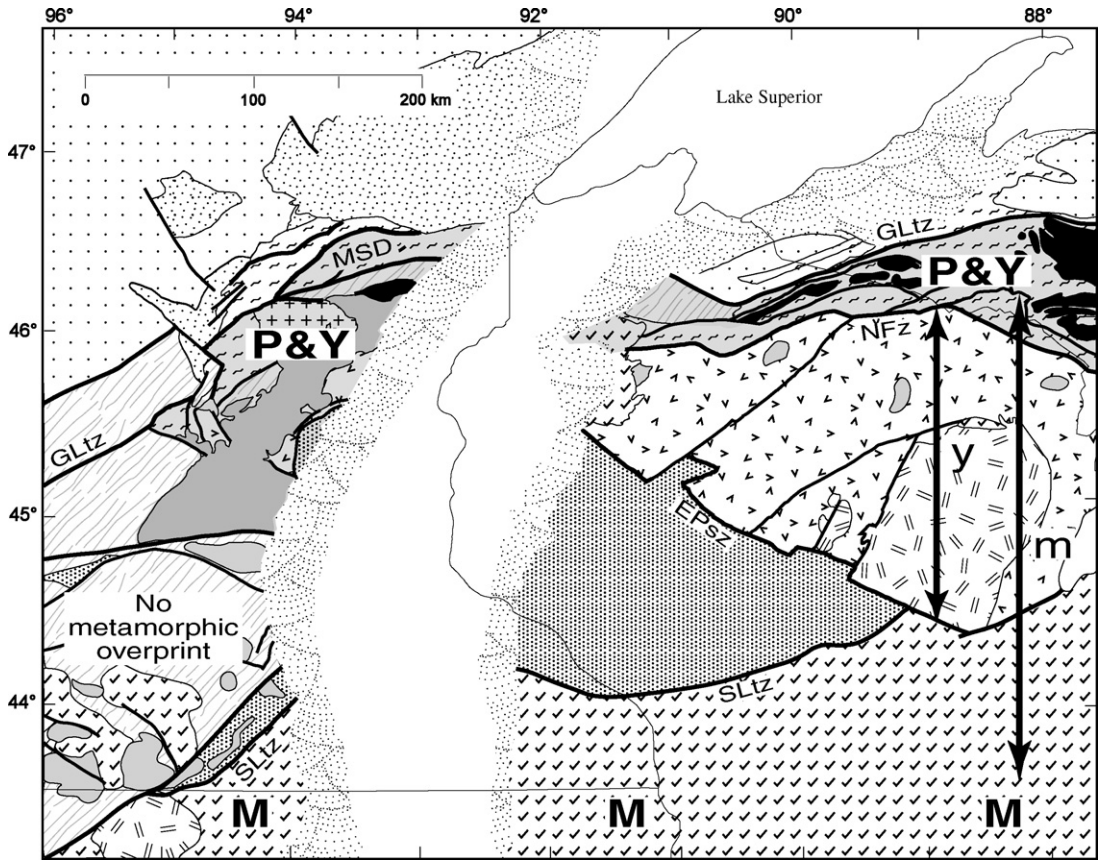

Fig. 7. Simplified geologic map of the southern Lake Superior region; see Fig. 2 for terrane description and geologic legend. Map denotes areas of dominant metamorphic effects associated with Paleoproterozoic accretionary events. "P&Y" (gray shaded area between GLtz and NFz) delineate amphibolite facies metamorphism related to Penokean and Yavapai accretion, respectively. "y" represents region of Yavapai greenschist facies metamorphism in Wisconsin, locally amphibolite facies adjacent to geon 17 plutons. "m" represents region of Mazatzal greenschist facies metamorphism in Wisconsin and southern part of upper peninsula of Michigan. "M" represents area of Mazatzal amphibolite facies metamorphism (in Iowa and southernmost Wisconsin south of the Baraboo quartzite). Note the absence of significant Paleoproterozoic metamorphic overprint in the Archean Minnesota River Valley block.

intruded over a 20 million years interval into midcrustal levels (ca. 15–18 km depths) shortly after peak orogenesis (Holm et al., 2005), all factors which favor a large metamorphic imprint. In contrast, rapid (<5 million years) emplacement of the Wolf River batholith (Dewane and Van Schmus, 2007) at shallow crustal levels long after cessation of orogeny are all likely factors in its limited metamorphic influence on the Proterozoic crust.

The cumulative metamorphic effect of late Paleoproterozoic accretionary tectonics in the southern Lake Superior region is depicted in Fig. 7. The southern continental margin rocks north of the Niagara fault zone underwent amphibolite facies metamorphism during Penokean orogenesis (P; Fig. 7). Penokean-interval orogenic crust experienced overprinting metamorphism related to two subsequent accretionary events which impinged on this region as Laurentia grew southward. Yavapai-interval accretion resulted in widespread amphibolite facies overprinting (Y; Fig. 7) and significant magmatism in the regions of greatest Penokean crustal thickening along the continental margin north of the main suture. Yavapai-interval greenschist facies metamorphism (y; Fig. 7) affected Penokean terrane rocks south of the Niagara fault zone. The effects of Mazatzal-interval metamorphism are restricted largely to the region south of the Penokean suture (an important exception being the Peavy area in northern Michigan) and are largely greenschist facies (m; Fig. 7). Mazatzal metamorphism reached amphibolite facies (M; Fig. 7) only further south in crust more proximal to the Mazatzal/Yavapai tectonic boundary (NICE working group, 2007; Van Schmus et al., 2007). The diminishing influence of superimposed metamorphic and plutonic events on the Proterozoic crust of the U.S. continental interior likely reflects the southward migration of the supercontinent's active margin during Laurentia's construction. Within only a few hundred million years of its accretion, the characteristics of a cratonized lithosphere appear to have been firmly established.

Acknowledgments

This research was funded by National Science Foundation grants EAR-9902704 and EAR-027432. We thank Mike Jercinovic at the University of Massachusetts for assistance with electron microprobe data collection, and Marty Grove at the University of California-Los Angeles for support with ion microprobe analyses. We are grateful to Peter Betts and an anonymous individual for providing thoughtful reviews and to Val Chandler for serving as guest editor. Terry Boerboom was extremely helpful in assisting with the collection of some of the Minnesota samples in the field.

Appendix A. Supplementary data

Supplementary data associated with this article can be found, in the online version, at doi:10.1016/j.precamres.2007.02.012.

References

Aldrich, L.T., Davis, G.L., James, H.L., 1965. Ages of some minerals from metamorphic and igneous rocks near Iron Mountain, Michigan. J. Petrol. 6, 445–472.

Allen, D.J., Hinze, W.J., 1992. Wisconsin gravity minimum: solution of a geologic and geophysical puzzle and implications for cratonic evolution. Geology 20, 515–518.

Anderson, R., 1983. Proterozoic anorogenic granite plutonism of North America. Geol. Soc. Am. Memoir 161, 133–152.

Attoh, K., Klasner, J., 1989. Tectonic implications of the metamorphism and gravity field in the Penokean orogen of northern Michigan. Tectonics 8, 911–933.

Cannon, W., Ottke, D., 2000. Preliminary digital geologic map of the Penokean (Early Proterozoic) continental margin in northern Michigan and Wisconsin. USGS Open-file report 99-547 (CD-ROM).

Catlos, E.J., Gilley, L.D., Harrison, M.T., 2002. Interpretation of monazite ages obtained via in situ analysis. Chem. Geol. 188, 193–215.

Cherniak, D.J., Watson, E.B., Grove, M., Harrison, T.M., 2004. Pb diffusion in monazite: a combined RBS/SIMS study. Geochim. Cosmochim. Acta 68, 829–840.

Coakley, B.J., Wang, H.F., 1992. Erosional amplification of flexural bulges—limits on acceptable interpretation applied to the Goodman Swell: Eos Trans. AGU 73, 571.

Cocherie, A., Legendre, O., Peucat, J., Kouamelan, A., 1998. Geochronology of polygentic monazites constrained by *in situ* electron microprobe Th–U–total Pb determinations: implications for Pb behavior in monazite. Geochim. Cosmochim. Acta 62, 2475–2497.

Dacre, G., Himmelberg, G., Morey, G., 1984. Pre-Penokean igneous and metamorphic rocks, Benton and Steams Cos., central Minnesota. Minn. Geol. Surv. Rept. Inv. 31, 16.

Dewane, T.J., Van Schmus, W.R., 2007. U–Pb geochronology of the Wolf River batholith, north-central Wisconsin: evidence for successive magmatism between 1484 Ma and 1470 Ma. Precambrian Res., this issue.

Dott Jr., R.H., 1983. The Proterozoic red quartzite enigma in the north central United States: resolved by plate collision? Geol. Soc. Am. Memoir 160, 129–141.

Foland, K.A., Flemming, T.H., Heimann, A., Elliot, D.H., 1993. Potassium-argon dating of fine grained basalts with massive Ar loss: Application of the $^{40}Ar/^{39}Ar$ technique to plagioclase and glass from the Kirkpatrick Basalt, Antarctica. Chem. Geo., Isot. Geosci. Sect. 107, 173–190.

Geiger, C., Guidotti, C., 1989. Precambrian metamorphism in the southern Lake Superior region and its bearing on crustal evolution. Geosci. Wisc. 13, 1–13.

Goldich, S.S., Nier, A.O., Baadsgaard, H., Hoffman, J.H., Krueger, H.W., 1961. The Precambrian Geology and geochronology of Minnesota. Minn. Geol. Surv. Bull. 41, 193.

Goldich, S.S., Hedge, C.E., Stern, T.W., 1970. Age of the Morton and Montevideo gneisses and related rocks, southwestern Minnesota. Geol. Soc. Am. Bull. 81, 3671–3696.

Goldich, S.S., 1968. Geochronology in the Lake Superior region. Can. J. Earth Sci. 5, 715–724.

Green, J.C., Bornhorst, T.J., Chandler, V.W., Mudrey, M.G., Jr., Myers, P.E., Pesonen, L.J., Wilband, J.T., 1987. Keweenawan dykes of the Lake Superior Region: evidence for Evolution of the Middle Proterozoic Midcontinent Rift of North America. In: Halls, Fahrig (Eds.), Mafic Dyke Swarms. Geol. Assoc. Canada Spec. Paper 34, pp. 289–302.

Hames, W.E., Hodges, K.V., 1993. Laser $^{40}Ar/^{39}Ar$ evaluation of slow cooling and episodic loss of ^{40}Ar from a sample of polymetamorphic muscovite. Science 261, 1721–1723.

Hanley, A.J., Kyser, T.K., Hiatt, E.E., Marlatt, J., Foster, S., 2006. The uranium mineralization potential of the Paleoproterozoic Sioux Basin and its relationship to other basins in the southern Lake Superior region. Precambrian Res. 148, 125–144.

Hodges, K.V., Bowring, S.A., 1995. $^{40}Ar/^{39}Ar$ thermochronology of isotopically zoned micas: insights from the southwestern USA Proterozoic orogen. Geochem. Cosmochim. Acta 59, 3205–3220.

Harrison, T.M., LeFort, P., McKeegan, K.D., 1995. Detection of inherited monazite in the Manaslu leucogranite by $^{208}Pb/^{232}Th$ ion microprobe dating; crystallization age and tectonic implications. Earth Planet. Sci. Lett. 133, 271–282.

Harrison, T.M., Grove, M., McKeegan, K.D., Coath, C.D., Lovera, O.M., Le Fort, P., 1999. Origin and emplacement of the Manaslu intrusive complex, Central Himalaya. J. Petrol. 40, 3–19.

Hoffman, P., 1989. Precambrian geology and tectonic history of North America. In: Bally, Palmer (Eds.), The Geology of North America—An Overview. GSA Decade of North America Geology A, pp. 478–480.

Holm, D.K., Lux, D., 1996. Core complex model proposed for gneiss dome development during collapse of the Paleoproterozoic Penokean orogen, Minnesota. Geology 24, 343–346.

Holm, D.K., Lux, D., 1998. Depth of emplacement and tilting of the Middle Proterozoic (1470 Ma) Wolf River batholith, Wisconsin: Ar–Ar thermochronologic constraints. Can. J. Earth Sci. 35, 1143–1151.

Holm, D.K., Selverstone, J., 1990. Rapid growth and strain rates inferred from synkinmatic garnets, Penokean orogen, Minnesota. Geology 18, 166–169.

Holm, D.K., Darrah, K., Lux, D., 1998a. Evidence for widespread ~1760 Ma metamorphism and rapid crustal stabilization of the Early Proterozoic Penokean orogen, Minnesota. Am. J. Sci. 298, 60–81.

Holm, D.K., Holst, T.B., Lux, D.R., 1993. Postcollisional cooling of the Penokean orogen in east-central Minnesota. Can. J. Earth Sci. 30, 913–917.

Holm, D., Schneider, D.A., Coath, C., 1998b. Age and deformation of Early Proterozoic quartzites in the southern Lake Superior region: implications for extent of foreland deformation during final assembly of Laurentia. Geology 26, 907–910.

Holm, D.K., Van Schmus, W.R., Mac Neil, L.C., Boerboom, T.J., Schweitzer, D., Schneider, D.A., 2005. U–Pb zircon geochronology of Paleoproterozoic plutons from the northern mid-continent, U.S.A.: evidence for subduction flip and continued convergence after geon 18 Penokean orogenesis. Geol. Soc. Am. Bull. 117, 259–275.

Holst, T.B., 1984. Evidence for nappe development during the Early Proterozoic Penokean Orogeny, Minnesota. Geology 12, 135–138.

James, H., 1955. Zones of regional metamorphism in the Precambrian of northern Michigan. Geol. Soc. Am. Bull. 66, 1455–1488.

Kelley, S.P., Turner, G., 1991. Laser probe $^{40}Ar–^{39}Ar$ measurements of loss profiles within individual hornblende grains from the Giants Range granite, northern Minnesota, USA. Earth Planet. Sci. Lett. 107, 634–648.

Karlstrom, K.E., Åhäll, K.-I., Harlan, S.S., Williams, M.L., McLelland, J., Geissman, J.W., 2001. Long-lived (1.8–1.0 Ga) convergent orogen in southern Laurentia, its extensions to Australia and Baltica, and implications for refining Rodinia. Precambrian Res. 111, 5–30.

King, E.R., 1990. Precambrian terrane of north-central Wisconsin: an aeromagnetic perspective. Can. J. Earth Sci. 27, 1472–1477.

Koppers, A.P., 2002. ArArCALC; software for Ar/Ar age calculations. Computers and Geosci. 28, 605–619.

Larue, D.K., 1983. Early Proterozoic tectonics of the Lake Superior region; tectonostratigraphic terranes near the purported collision zone. Geol. Soc. Am. Memoir 160, 33–47.

Marshak, S., Tinkham, D., Alkmim, F., Brueckner, H., Bornhorst, T., 1997. Dome and keel provinces formed during the Paleoproterozoic orogenic collapse–core complexes, diapirs, or neither?: examples from the Quadrilatero Ferrifero and the Penokean orogen. Geology 25, 415–418.

Medaris, G., Singer, B.S., Dott Jr., R.H., Naymark, A., Johnson, C.M., Schott, R.C., 2003. Late Paleoproterozoic climate, tectonics and metamorphism in the southern Lake Superior region and Proto-North America: evidence from Baraboo Interval quartzites. J. Geol. 111, 243–257.

Montel, J.-M., Foret, S., Veschambrem, M., Nicollet, C., Provost, A., 1996. Electron microprobe dating of monazite. Chem. Geol. 131, 37–53.

NICE working group, 2007. Reinterpretation of Paleoproterozoic accretionary boundaries of the north-central United States based on a new aeromagnetic-geologic compilation. Precambrian Res. 157, 71–79.

Peterman, Z.E., 1966. Rb–Sr dating of Middle Precambrian metasedimentary rocks, Minnesota. Geol. Soc. Am. Bull. 77, 1031–1044.

Peterman, Z.E., Sims, P.K., 1988. The Goodman Swell: a lithospheric flexure caused by crustal loading along the Mid-continent Rift system. Tectonics 7, 1077–1090.

Pouchou, J., Pichoir, F., 1984. A new model for quantitative X-ray microanalysis. Part I. Application to the analysis of homogeneous samples. La Rech. Aerospatiale 3, 13–38.

Pouchou, J., Pichoir, F., 1985. "PAP" phi-rho-Z procedure for improved quantitative microanalysis. In: Armstrong, J. (Ed.), Microbeam Analysis. San Francisco Press Inc., San Francisco, pp. 104–106.

Renne, P., Swisher, C., Deino, A., Karner, D., Owens, T., DePaolo, D., 1998. Intercalibration of standards, absolute ages and uncertainties in $^{40}Ar/^{39}Ar$ dating. Chem. Geol. 145, 117–152.

Rogers, J.J.W., Dabbagh, M.E., Olszewski Jr., W.J., Gaudette, H.E., Greenberg, J.K., Brown, B., 1984. Early poststabilization sedimentation and later growth of shields. Geology 12, 607–609.

Romano, D., Holm, D.K., Foland, K., 2000. Determining the extent and nature of Mazatzal-related overprinting of the Penokean orogenic belt in the southern Lake Superior region, north-central USA. Precambrian Res. 104, 25–46.

Rose, S., 2004. The Age and Extent of Metamorphism Within the Paleoproterozoic Penokean Orogen, Northern Wisconsin and Michigan. M.S. Thesis. Ohio University, 105 p.

Schneider, D.A., Holm, D.K., Lux, D., 1996. On the origin of Early Proterozoic gneiss domes and metamorphic nodes, northern Michigan. Can. J. Earth Sci. 33, 1053–1063.

Schneider, D.A., Bickford, M.E., Cannon, W., Shulz, K., Hamilton, M., 2002. Age of volcanic rocks and syndepositional iron formations, Marquette Range Supergroup: implications for the tectonic setting of Paleoproterozoic iron formations of the Lake Superior region. Can. J. Earth Sci. 39, 999–1012.

Schneider, D.A., Holm, D.K., O'Boyle, C., Hamilton, M., Jercinovic, M., 2004. Paleoproterozoic development of a gneiss dome corridor in the southern Lake Superior region, USA: In: Whitney, et al. (Eds.), Gneiss Domes in Orogeny: Geol. Soc. Am. Special Paper 380, pp. 339–357.

Sims, P., Van Schmus, R., Schulz, K., Peterman, Z., 1989. Tectonostratigraphic evolution of the Early Proterozoic Wisconsin magmatic terranes of the Penokean orogen. Can. J. Earth Sci. 26, 2145–2158.

Southwick, D., Morey, G., McSwiggen, P., 1988. Geologic map of the Penokean orogen, central and eastern Minnesota and accompanying text. MGS Rept. Inv. 37, 1:250,000.

Stonier, P., 2006. EMPA Dating of Monazite From Metaquartzites and Metapelites, Southern Wisconsin. M.S. Thesis. Kent State University, 66 p.

Suzuki, K., Adachi, M., 1991. Precambrian provenance and Silurian metamorphism of the Tsubonosawa paragneiss in the South Kitakami terrane, NE Japan, revealed by the chemical Th–U–total Pb isochron ages of monazite, zircon, and xenotime. Geochem. J. 25, 357–376.

Tinkham, D.K., Marshak, S., 2004. Precambrian dome-and-keel structure in the Penokean orogenic belt of northern Michigan, USA. In: Whitney, et al. (Eds.), Gneiss Domes in Orogeny: Geol. Soc. Am. Special Paper 380, pp. 321–338.

Tohver, E., Holm, D.K., van der Pluijm, B.A., Essene, E.J., Cambray, F.W., 2007. Late Paleoproterozoic (geon 18 and 17) reactivation of the Neoarchean Great Lakes tectonic zone, northern Michigan, USA: evidence from kinematic analysis, thermobarometry, and Ar/Ar geochronology. Precambrian Res. 157, 144–168.

Townsend, K.J., Miller, C.F., D'Andrea, J.L., Ayers, J.C., Harrison, T.M., Coath, C.D., 2000. Low temperature replacement of monazite in the Ireteba granite, Southern Nevada: geochronological implications. Chem. Geol. 172, 95–112.

Van Schmus, W.R., 1976. Early and Middle Proterozoic history of the Great Lakes area, North America. Royal Soc. Lond. Philos. Trans. 280, 605–628.

Van Schmus, W.R., 1980. Chronology of igneous rocks associated with the Penokean orogeny in WI. In: Morey, Hanson (Eds.), Selected studies of Archean gneisses and lower Proterozoic rocks, southern Canadian Shield. Geol. Soc. Am. Spec. Paper 182, pp. 159–168.

Van Schmus, W.R., Woolsey, L.L., 1975. Rb/Sr geochronology of the Republic Area, Marquette County, Michigan. Can. J. Earth Sci. 12, 1723–1733.

Van Schmus, R., Bickford, M.E., Condie, K., 1993. Early Proterozoic crustal evolution. In: Reed, et al. (Eds.), Precambrian: Conterminous U.S. GSA Decade of North America Geology C-2, pp. 270–281.

Van Schmus, W.R., Schneider, D.A., Holm, D.K., Dodson, S., Nelson, B.K., 2007. New insights into the southern margin of the Archean–Proterozoic transition in the north-central U.S. based on U–Pb, Sm–Nd, and Ar–Ar geochronology. Precambrian Res., this issue.

Williams, M.L., Jercinovic, M.J., 2002. Microprobe monazite geochronology: putting absolute time into microstructural analysis. J. Struct. Geol. 24, 1013–1028.

Williams, M.L., Jercinovic, M.J., Terry, M.P., 1999. Age mapping and dating of monazite on the electron microprobe: deconvoluting multistage tectonic histories. Geology 27, 1023–1026.